

Large Field Polynomial Inflation: Parameter Space, Predictions and (Double) Eternal Nature

Manuel Drees^a and Yong Xu^{a,b}

^a*Bethe Center for Theoretical Physics and Physikalisches Institut, Universität Bonn,
Nussallee 12, 53115 Bonn, Germany*

^b*PRISMA+ Cluster of Excellence and Mainz Institute for Theoretical Physics, Johannes
Gutenberg University, 55099 Mainz, Germany¹*

E-mail: drees@th.physik.uni-bonn.de, yongxu@th.physik.uni-bonn.de,
yongxu@uni-mainz.de

Abstract. Simple monomial inflationary scenarios have been ruled out by recent observations. In this work we revisit the next simplest scenario, a single-field model where the scalar potential is a polynomial of degree four which features a concave “almost” saddle point. We focus on trans-Planckian field values. We reparametrize the potential, which greatly simplifies the procedure for finding acceptable model parameters. This allows for the first comprehensive scan of parameter space consistent with recent Planck and BICEP/Keck 2018 measurements. Even for trans-Planckian field values the tensor-to-scalar ratio r can be as small as $\mathcal{O}(10^{-8})$, but the model can also saturate the current upper bound. In contrast to the small-field version of this model, radiative stability does not lead to strong constraints on the parameters of the inflaton potential. For very large field values the potential can be approximated by the quartic term; as well known, this allows eternal inflation even for field energy well below the reduced Planck mass M_{Pl} , with Hubble parameter $H \sim 10^{-2} M_{\text{Pl}}$. More interestingly, we find a region of parameter space that even supports *two phases of eternal inflation*. The second epoch only occurs if the slope at the would-be saddle point is very small, and has $H \sim 10^{-5} M_{\text{Pl}}$; it can only be realized if $r \sim 10^{-2}$, within the sensitivity range of next-generation CMB observations.

¹Address after December 1, 2022.

Contents

1	Introduction and Motivation	1
2	The Setup	3
2.1	General Analysis	3
2.2	Approximations	6
3	Model Parameters and Predictions	9
3.1	Method to Find Model Parameters and Examples	9
3.2	Complete Scan of Parameter Space	11
4	Radiative Stability and Reheating	15
4.1	Reheating	15
5	Eternal Polynomial Inflation	16
5.1	Eternal Phase I	17
5.2	Eternal Phase II	18
6	Summary and Conclusions	19
A	General Expression for the Number of e-Folds	23

1 Introduction and Motivation

Inflation, as invented in the 1980s [1–4], is an elegant paradigm of early universe physics. It not only solves the horizon, flatness and monopole problems of standard cosmology, but also generates initial seeds for structure formation arising from vacuum fluctuations [5]. In the simplest, “slow-roll” implementation of this idea, a spin-0 inflaton field is introduced which slowly rolls down a sufficiently flat potential; see Ref. [6] for a comprehensive review of models of inflation.

The simplest model assumes a monomial ϕ^p potential; in renormalizable models whose potential is bounded from below p is either 2 or 4. However, such potentials are sufficiently flat, i.e. the first and second derivatives of the potential are sufficiently small compared to the potential itself, only at large field values. This leads to the overproduction of tensor modes, i.e. the tensor-to-scalar ratio r is predicted beyond the upper bound established by recent measurements of Cosmic Microwave Background (CMB) anisotropies [7, 8].¹

In this paper, we still assume that the inflaton is a real scalar field ϕ , but we allow a general, renormalizable polynomial potential. This next to simplest scenario has been analyzed many times since 1990 [11–20]. Such polynomial inflation can also be realized in string theory [21]. All these analyses have been performed before the release of the 2018 Planck and BICEP/Keck results [7, 8]. Unlike previous investigations, we aim to work out the full parameter space that agrees with the latest measurements, and derive the allowed

¹One may also consider monomials with fractional power, e.g. the monodromy inflationary model where $V(\phi) \propto \phi^{2/3}$ [9, 10]. The BICEP/Keck 2018 results [8] then require $p < 0.53$ at 95% c.l. if CMB scales experienced no more than 60 e-folds of inflation, in strong tension with monodromy inflation.

range of r . This is timely since future precise observations, for example by CORE [22], AliCPT [23], LiteBIRD [24], and CMB-S4 [25], should greatly extend the sensitivity, down to $r \sim \mathcal{O}(10^{-3})$.

As noted above, the potential should be flatter than a monomial at not too large field values. Here we achieve this by canceling several contributions, with different powers of the field, around a (near) saddle point, where both the first and second derivative of the potential become small. This is similar to the inflection point inflationary scenario [26–32]; however, we employ a purely renormalizable potential, i.e. only allow terms up to ϕ^4 . Just below the would-be saddle point the potential has a concave shape, as favored by the Planck 2018 data [7]. We rewrite the potential in terms of the location ϕ_0 of the would-be saddle point, a quantity β which governs the slope of the potential at ϕ_0 , and a multiplicative factor which only affects the overall normalization of the CMB anisotropies. Based on this reparametrization, we work out, for the first time, the full parameter space with predictions (power spectrum, spectral index and its running) consistent with Planck and BICEP/Keck 2018 measurements [7]. We find that the current upper bound on r can be saturated, which means that part of the parameter space should be testable in the near future.

Another aim of this work is to investigate at which scale(s) eternal inflation² might have occurred. In slow-roll inflation the classical change of the inflaton field during one Hubble time dominates over its quantum fluctuation; the inflaton field thus moves essentially deterministically downhill towards its minimum, until the end of inflation. However, in the opposite situation, where the quantum fluctuations dominate over the classical evolution, the inflaton field can move uphill rather than downhill. The Hubble patches where this happens inflate longer; in fact, in this case some such patches will inflate forever, i.e. inflation becomes eternal, although in our patch inflation obviously must have ended. The possibility that inflation can be eternal was first discussed in Ref. [34]. Later it was shown [35] that eternal inflation is in fact inevitable if the potential is a monomial with positive power, assuming only that the initial field value is sufficiently large; this occurs at energy scales well below the reduced Planck mass, $M_{\text{Pl}} \simeq 2.4 \cdot 10^{18}$ GeV. One thus may not need to worry about quantum gravity effects when describing eternal inflation [36]. “Hilltop” models can also lead to eternal inflation [37, 38].

During the eternal expansion, infinitely many independent “mini-universes” (or “pocket universes”) with different de Sitter vacua are generated via a self-reproducing process [39]. It has been speculated that this process can “populate” (or probe) the landscape of string theory [40–42]. This mechanism also naturally provides a scientific justification for the (weak) anthropic principle. From the perspective of eternal inflation, nearly everything is possible, provided only that the overall energy density is dominated by the potential energy of the inflaton field. For example, independent mini-universes may feature different types of compactification leading to different fundamental physical laws and/or different values of physical “constants” (which are field-dependent in superstring theory). Some of these laws and constants support life of our type, and clearly we (as living beings) can only observe those mini-universes where this is indeed the case [39, 43]. Finally, eternal inflation may help to relax the initial conditions problem. By this we mean the probability that some initial configuration of the inflaton field, and of the other dynamical degrees of freedom, gives rise to sufficiently long exponential expansion of the universe.³ As argued in [46], any

²See e.g. Ref. [33] for a review.

³For a review see e.g. Refs. [44, 45].

initial configuration that leads to eternal inflation will produce an infinite spacetime volume, making the probability of this initial configuration less significant.

Since for large field values our potential is dominated by the ϕ^4 term, it is not surprising that it leads to eternal inflation at sufficiently large values of ϕ ; the minimal required inflaton field energy turns out to be slightly lower than in pure ϕ^4 inflation. More intriguingly, for sufficiently small values of β , i.e. a sufficiently flat potential near the would-be saddle point, a second period of eternal inflation can occur, at a value of the Hubble parameter smaller by more than three orders of magnitude than that during the first epoch of eternal inflation. However, this can only be realized if $\phi_0 \gtrsim 15M_{\text{Pl}}$, with $r \gtrsim 0.01$. These scenarios can therefore be probed in the near future.

The remainder of this paper is organized as follows. In sec. 2 we describe the general setup, with emphasis on the reparametrization of the inflaton potential. In sec. 3 methods to scan the allowed parameter space are shown, and the corresponding predictions are given. The radiative stability of the potential is checked and the maximal reheating temperature is determined in sec. 4. In sec. 5 we investigate the possibility of realizing eternal inflation in our scenario, with focus on the calculation of the corresponding energy scale(s). Finally, sec. 6 summarizes this work. In this paper, we use Planckian units, i.e. we set the reduced Planck mass $M_{\text{Pl}} = \sqrt{\frac{1}{8\pi G}} \simeq 2.4 \cdot 10^{18}$ GeV to unity.

2 The Setup

In this section we first describe the inflaton potential and the resulting expressions for the parameters of inflation; in the second subsection we present simplified analytical results in some limits.

2.1 General Analysis

The action for the inflaton field in the Einstein frame is given by:

$$S = \int d^4x \sqrt{-g} \left[\frac{1}{2} g_{\mu\nu} \partial^\mu \phi \partial^\nu \phi - V(\phi) \right], \quad (2.1)$$

where g is the determinant of the metric; we assume it to be of the Friedmann–Robertson–Walker (FRW) type, i.e. $g_{\mu\nu} = \text{diag}(+1, -a^2, -a^2, -a^2)$ with a denoting the scale factor. The corresponding Euler–Lagrange equation of motion for the classical background field is

$$\ddot{\phi} + 3H\dot{\phi} - \frac{1}{a^2} \nabla^2 \phi + V'(\phi) = 0. \quad (2.2)$$

Here $\vec{\nabla}$ denotes derivatives with respect to comoving spatial coordinates, and $H \equiv \frac{\dot{a}}{a}$ is the Hubble parameter, which is determined by the Friedmann equation:

$$H^2 = \frac{1}{3} \rho(\phi) = \frac{1}{3} \left[\frac{1}{2} (\dot{\phi})^2 + V(\phi) + \frac{1}{2a^2} (\nabla\phi)^2 \right]. \quad (2.3)$$

We make the usual assumption that the classical background ϕ is homogeneous, i.e. $\phi \equiv \phi(t)$ is a function of the cosmic time t only, so that all gradient terms for the background field vanish. The potential we are considering is the general renormalizable one⁴:

$$V(\phi) = b\phi^2 + c\phi^3 + d\phi^4. \quad (2.4)$$

⁴A linear term can be removed through a shift of ϕ . We neglect the tiny cosmological constant term, which would be generated by a constant term in the potential.

We need $d > 0$ for the potential to be bound from below, and we consider $b > 0$ so that the minimum of the potential is at $\phi = \phi_{\min} = 0$, with $V(\phi_{\min}) = 0$. Since the potential is symmetric under the transformation $c \rightarrow -c$, $\phi \rightarrow -\phi$, we set $c \leq 0$ without loss of generality, so that inflation occurs at positive field values.⁵ The first and second derivatives of the potential are given by:

$$V'(\phi) = 2b\phi + 3c\phi^2 + 4d\phi^3; \quad V''(\phi) = 2b + 6c\phi + 12d\phi^2. \quad (2.5)$$

We need the potential to be very flat over some range of field values. Suppose first that the potential features an exact saddle point at $\phi = \phi_0$, i.e. $V'(\phi_0) = V''(\phi_0) = 0$, which requires

$$\phi_0 = -\frac{3c}{8d}; b = \frac{9c^2}{32d}, \quad (2.6)$$

from which we learn that the ratio c/d determines the position of the saddle point. Allowing for a finite slope even at ϕ_0 , one can reparametrize the potential as

$$\begin{aligned} V(\phi) &= d \left[\phi^4 + \frac{c}{d} (1 - \beta) \phi^3 + \frac{9}{32} \left(\frac{c}{d} \right)^2 \phi^2 \right] \\ &= d \left[\phi^4 + A (1 - \beta) \phi^3 + \frac{9}{32} A^2 \phi^2 \right]. \end{aligned} \quad (2.7)$$

Here $A \equiv \frac{c}{d} \equiv -\frac{8}{3}\phi_0$ determines the location of the flat region of the potential. Note that the potential (2.7) still contains three free parameters, d , A and β , i.e. it is a genuine reparametrization of the general ansatz (2.4). However, the form (2.7) is far more convenient, since the overall multiplicative factor d only affects the overall normalization of the density perturbations, while β directly controls the slope near ϕ_0 . For $\beta < 0$ the potential has a second minimum at $\phi > \phi_0$ where the inflaton field may get stuck, in which case there would be no hot Big Bang. We therefore require $\beta \geq 0$; recall that for $\beta = 0$ the potential has an exact saddle point at ϕ_0 .

In this paper, we focus on the large field inflation scenario where $\phi_0 \geq 1$; a detailed analysis of the small field case can be found in Ref. [49].

The traditional potential slow-roll (SR) parameters [50] are:

$$\begin{aligned} \epsilon_V &\equiv \frac{1}{2} \left(\frac{V'}{V} \right)^2 = \frac{2}{\phi^2} \left[\frac{9A^2 - 48A(\beta - 1)\phi + 64\phi^2}{9A^2 - 32A(\beta - 1)\phi + 32\phi^2} \right]^2; \\ \eta_V &\equiv \frac{V''}{V} = \frac{6}{\phi^2} \left[\frac{3A^2 - 32A(\beta - 1)\phi + 64\phi^2}{9A^2 - 32A(\beta - 1)\phi + 32\phi^2} \right]; \\ \xi_V^2 &\equiv \frac{V'V'''}{V^2} = -\frac{384[A(\beta - 1) - 4\phi]}{\phi^3} \frac{(9A^2 - 48A(\beta - 1)\phi + 64\phi^2)}{(9A^2 - 32A(\beta - 1)\phi + 32\phi^2)^2}. \end{aligned} \quad (2.8)$$

These quantities do not depend on d . During SR inflation, all these parameters must be small, ϵ_V , $|\eta_V|$ and $|\xi_V^2| \ll 1$.

Inflation ends at a field value ϕ_{end} where $\epsilon_V(\phi_{\text{end}}) = 1$. Since for $\phi \ll \phi_0$ the term $9A^2 = 64\phi_0^2$ dominates over other terms in eq. (2.8), $\epsilon_V \approx 2/\phi^2 \approx \eta_V$ and hence $\phi_{\text{end}} \approx 1.41$

⁵The simpler case with $c = 0$, so that the potential has only two terms, has been investigated in Ref. [47]; our analysis shows that this scenario is no longer viable. In Ref. [48], the two-term scenario with radiative corrections is investigated.

if $\phi_0 \gg 1$. For smaller ϕ_0 , ϕ_{end} is closer to ϕ_0 so that the cubic and quartic terms need to be included in its determination.

Another important quantity is the total number N_{CMB} of e-folds of inflation that occurred after the CMB pivot scale $k_\star = 0.05\text{Mpc}^{-1}$ first crossed out the horizon; in our model it can be computed analytically (within the SR approximation). The full result is given in the Appendix; for $\beta \ll 1$ it reduces to

$$N_{\text{CMB}} = \int_{\phi_{\text{end}}}^{\phi_{\text{CMB}}} \frac{1}{\sqrt{2\epsilon_V}} d\phi \simeq \frac{1}{24} \left\{ 3\phi^2 - 4\phi\phi_0 + 15\phi_0^2 - \phi_0^2 \sqrt{\frac{2}{\beta}} \arctan\left(\frac{\phi_0 - \phi}{\sqrt{2\beta}\phi_0}\right) - \phi_0^2 \ln[(\phi_0 - \phi)^2] \right\} \Big|_{\phi_{\text{end}}}^{\phi_{\text{CMB}}}. \quad (2.9)$$

Here ϕ_{CMB} denotes value of the field when k_\star crossed out of the horizon. In order to solve the flatness and horizon problems, $\gtrsim 50$ e-folds of inflation are needed.

During SR inflation with a quasi de Sitter spacetime, Gaussian curvature perturbations are generated, with power [50]

$$\mathcal{P}_\zeta = \frac{V}{24\pi^2\epsilon_V}. \quad (2.10)$$

The spectral index n_s and its running α are given by

$$n_s = 1 - 6\epsilon_V + 2\eta_V; \quad \alpha = 16\epsilon_V\eta_V - 24\epsilon_V^2 - 2\xi_V^2; \quad (2.11)$$

measurements of these quantities can be used to constrain the model parameters β and A .

The final observable of interest is the tensor-to-scalar ratio r , which is given by [50]

$$r = 16\epsilon_V = \frac{32}{\phi^2} \left[\frac{9A^2 - 48A(\beta - 1)\phi + 64\phi^2}{9A^2 - 32A(\beta - 1)\phi + 32\phi^2} \right]^2. \quad (2.12)$$

The final Planck 2018 measurements at the pivot scale $k_\star = 0.05\text{Mpc}^{-1}$, including their own measurements plus results on baryonic acoustic oscillations (BAO), give in a 7 parameter cosmological model (baseline ΛCDM plus running n_s) [7]:

$$\mathcal{P}_\zeta = (2.1 \pm 0.1) \cdot 10^{-9}; \quad n_s = 0.9659 \pm 0.0040; \quad \alpha = -0.0041 \pm 0.0067. \quad (2.13)$$

So far no evidence for a non-vanishing tensor-to-scalar ratio r has been found. The most recent upper bound, from BICEP/Keck 2018 results [8], is

$$r_{0.05} < 0.035 \quad (2.14)$$

at 95% C.L., after extrapolation to our pivot scale.⁶

The combined constraint on r and n_s (adapted from Ref. [8]) is shown in Fig. 1. We also present predictions for three sets of free parameters of the potential (2.7), chosen such that $\mathcal{O}(10^{-3}) \lesssim r \lesssim \mathcal{O}(10^{-2})$, which should be testable in the near future [22–25].

⁶Note that in the experimental literature (e.g. the $r - n_s$ plots of Planck [7] or BICEP/Keck [8]) the bound on r is usually quoted at scale $k = 0.002\text{Mpc}^{-1}$, denoted by $r_{0.002}$. For our choice of the pivot scale $k_\star = 0.05\text{Mpc}^{-1}$, one has $r_{0.05} \simeq r_{0.002} \left(\frac{0.05}{0.002}\right)^{n_T} \simeq r_{0.002} \left(\frac{0.05}{0.002}\right)^{-r_{0.002}/8}$, where the (small) running of the tensor spectral index $n_T \simeq -r/8$ has been neglected.

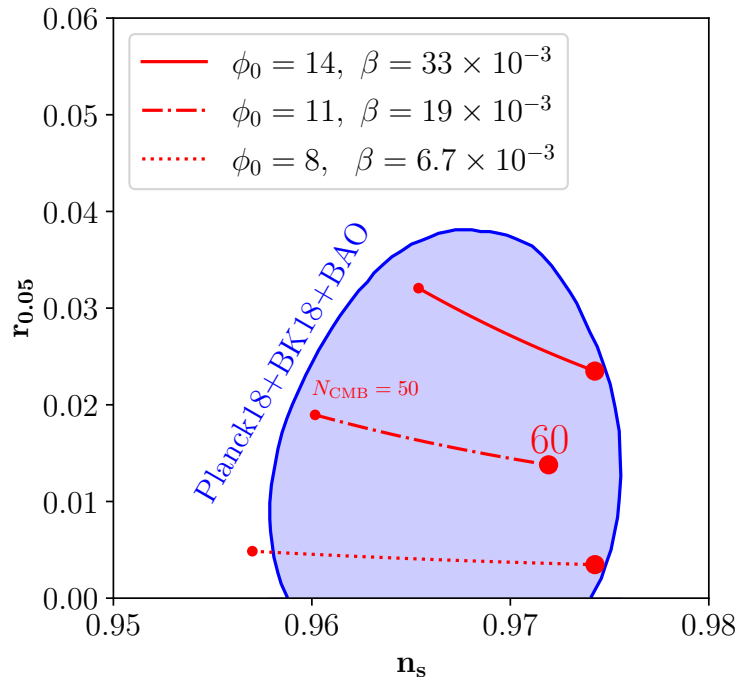


Figure 1: The blue shaded region is the currently allowed part of the $r-n_s$ plane; it has been adapted from the recent BICEP/Keck 2018 results [8]. The red lines show predictions for our model, defined in eq.(2.7), where the parameters have been chosen such that $\mathcal{O}(10^{-3}) \lesssim r \lesssim \mathcal{O}(10^{-2})$. The small and big red dots correspond to $N_{\text{CMB}} = 50$ and 60, respectively.

2.2 Approximations

Eqs.(2.8) to (2.12) allow a fully analytical calculation of all SR parameters in terms of the free parameters of the potential plus the value of ϕ_{CMB} , which is also a free parameter. However, these equations are too complicated to be solved analytically for the free parameters, for given n_s , α and N_{CMB} . In this section, we therefore present simplified analytical expressions, which work well in some limits.

1. $\phi \approx \phi_0$:

In this regime, analytical results for the inflationary predictions can be obtained by rewriting the field as [49]

$$\phi = \phi_0(1 - \delta). \quad (2.15)$$

Decreasing ϕ corresponds to increasing δ . Note that fluctuations at scales probed by observations of the CMB must have been created at $\phi < \phi_0$, where the inflaton potential is concave, i.e. $\eta_V < 0$, so that $n_s < 1$ can be reproduced. Since both δ and β are rather small (as we will see, $\delta \gtrsim \mathcal{O}(\sqrt{\beta})$ is needed, so that $\beta \ll \delta \ll 1$), it will be sufficient to keep only terms linear in β and up to quadratic in δ in the analysis.

The SR parameters defined in (2.8) can then be approximated as [49]:

$$\epsilon_V \simeq \frac{72(2\beta + \delta^2)^2}{\phi_0^2}; \quad \eta_V \simeq \frac{24(2\beta - \delta)}{\phi_0^2}; \quad \xi_V^2 \simeq \frac{288(2\beta + \delta^2)}{\phi_0^4}. \quad (2.16)$$

Using the simplified result for ϵ_V , the number of e-folds becomes [49]

$$\begin{aligned}
N_{\text{CMB}} &= \int_{\phi_{\text{end}}}^{\phi_{\text{CMB}}} \frac{1}{\sqrt{2\epsilon_V}} d\phi \\
&= -\frac{\phi_0^2}{12} \int_{\delta_{\text{end}}}^{\delta_{\text{CMB}}} \frac{d\delta}{(2\beta + \delta^2)} \\
&\simeq \frac{\phi_0^2}{12\sqrt{2\beta}} \left[\frac{\pi}{2} - \arctan\left(\frac{\delta_{\text{CMB}}}{\sqrt{2\beta}}\right) \right].
\end{aligned} \tag{2.17}$$

The normalization of the power spectrum, its spectral index and the running of the spectral index defined in (2.11), simplify to [49]

$$\mathcal{P}_\zeta \simeq \frac{d\phi_0^6}{5184\pi^2(\delta^2 + 2\beta)^2}; \tag{2.18}$$

$$n_s \simeq 1 - \frac{48\delta}{\phi_0^2}; \tag{2.19}$$

$$\alpha \simeq -\frac{576(2\beta + \delta^2)}{\phi_0^4}. \tag{2.20}$$

Finally, the tensor-to-scalar ratio r defined in eq.(2.12) reduces to [49]

$$r \simeq \frac{1152(2\beta + \delta^2)^2}{\phi_0^2}. \tag{2.21}$$

Evidently eq.(2.19) immediately determines δ , i.e. ϕ_{CMB} . β can then be fixed using eq.(2.17): the argument of the arctan needs to be $\mathcal{O}(1)$, giving $\beta \sim \mathcal{O}(\delta^2)$, as claimed above. Moreover, $|\eta_V| \gg \epsilon_V$ in this scenario. The SR conditions thus cease to be satisfied at $\phi_{\text{end}} \simeq \phi_0(1 - \phi_0^2/24)$, where η_V crosses -1 [49]. However, exponential expansion continues until $\epsilon_V \simeq 1$, which is satisfied for $\phi \simeq \phi_0 \left(1 - \sqrt{\phi_0/(6\sqrt{2})}\right)$.

In ref.[49] it was shown that this approximation works very well for $\phi_0 \leq 1$. Here we find that it still works quite well even for $\phi_0 \lesssim 5$.

2. $\phi \gg \phi_0$:

Here the potential is dominated by the quartic term:

$$V \simeq d\phi^4. \tag{2.22}$$

The corresponding SR parameters are:

$$\epsilon_V = \frac{8}{\phi^2}; \quad \eta_V = \frac{12}{\phi^2}, \tag{2.23}$$

while the spectral index is given by

$$n_s = 1 - 6\epsilon_V + 2\eta_V = 1 - \frac{24}{\phi^2}. \tag{2.24}$$

The Planck central value $n_s = 0.9659$ (cf. eq.(2.13)) thus requires $\phi_{\text{CMB}} \simeq 27$, which implies $r = \frac{128}{\phi^2} \simeq 0.18$. This is well above the current upper bound on r , see fig. 1. Moreover, $\phi_{\text{CMB}} = 27$ with a ϕ^4 potential yields $N_{\text{CMB}} \simeq 90$, which is also well above the allowed range. This re-derives the by now quite well-known result that simple ϕ^4 inflation is excluded; as we noted in the Introduction, this holds for any monomial inflaton potential, $V(\phi) \propto \phi^p$ with $p \geq 2$.

3. $\phi \gtrsim \phi_0$:

If ϕ is very close to ϕ_0 the first approximation can again be used, but now with $\delta < 0$. Eq.(2.19) shows that then $n_s > 1$ if $\beta \ll 1$, in conflict with observation. Solutions with $\phi_{\text{CMB}} > \phi_0$ require larger values of β than those with $\phi_{\text{CMB}} < \phi_0$ in order to keep N_{CMB} within the acceptable range. In fact, for $\beta > 0.1$, $n_s < 1$ even for $\phi_{\text{CMB}} = \phi_0$, since $6\epsilon_V > 2\eta_V$ then. However, for $\phi_{\text{CMB}} = \phi_0$ and $\beta = 0.1$ one has $r = 128/(9\phi_0^2)$. $r < 0.035$ then requires $\phi_0 > 20$, which in turn yields⁷ $N_{\text{CMB}} > 150$. In order to obtain a value of n_s close to its upper bound (2.13) at $\phi_{\text{CMB}} = \phi_0$ one even needs $\beta \gtrsim 0.2$; $r < 0.035$ then requires $\phi_0 > 28$ and $N_{\text{CMB}} > 245$, about a factor of 4 above the desired range.

In the regime with $\phi > \phi_0$ but neither $\phi \sim \phi_0$ nor $\phi \gg \phi_0$, the potential remains convex, i.e. $\eta_V > 0$. As for the case $\phi_{\text{CMB}} \simeq \phi_0$ one can still get $n_s < 1$, since for sufficiently large β and/or ϕ_{CMB} ϵ_V becomes larger than $\eta_V/3$. However, once again this leads to too large values for N_{CMB} or r (or both). Therefore *no* viable solution with $\phi_{\text{CMB}} \geq \phi_0$ exists.

4. $\phi \ll \phi_0$:

If $\phi \ll \phi_0$, the quadratic term in the potential (2.7) dominates:

$$V(\phi) \simeq b\phi^2. \quad (2.25)$$

The corresponding SR parameters are

$$\epsilon_V = \frac{2}{\phi^2} = \eta_V, \quad (2.26)$$

giving a spectral index

$$n_s = 1 - 6\epsilon_V + 2\eta_V = 1 - \frac{8}{\phi^2}. \quad (2.27)$$

The central value (2.13) of n_s measured by Planck 2018 is reproduced for $\phi_{\text{CMB}} \simeq 15$, which in turn leads to $r \simeq 0.14$, well above its upper bound. ($N_{\text{CMB}} \simeq 56$ comes out correctly in this case.)

5. $\phi < \phi_0$:

In the regime with $\phi < \phi_0$ but with ϕ_{CMB} neither close to ϕ_0 nor $\phi_{\text{CMB}} \ll \phi_0$, the potential can maintain a small and *negative* curvature due to the negative contribution from the cubic term slightly overcompensating the positive contributions from the quadratic and quartic terms. In fact, for $\beta \ll 1$ the potential remains concave for

⁷For such large values of β eq.(2.9) is no longer valid, and the full expression given in the Appendix should be used.

$\phi_0(1 - 2\beta) > \phi > \phi_0(1 + 2\beta)/3$. If $\phi_0 \lesssim 1$, $|\eta_V|$ begins to exceed 1, signaling the end of SR inflation, already at a value of ϕ close to ϕ_0 , see eq.(2.16). However, for $\phi_0 > 1$ SR inflation can extend to field values well below ϕ_0 . In fact for very large ϕ_0 , the potential is effectively approaching a quadratic one again, since the last $\lesssim 65$ e-folds of inflation happen at $\phi \ll \phi_0$; this leads back to the case discussed in the previous paragraph, which is excluded by the upper bound on r . This argument shows that there must be an upper bound on ϕ_0 in our model. In the remainder of this paper we will explore the parameter space with $\phi_0 > 1$ and $\phi_{\text{CMB}} < \phi_0$ in detail.

3 Model Parameters and Predictions

In this section, we first describe our methods to search for acceptable model parameters and then scan over the full parameter space that is consistent with the latest CMB observations (2.13) and (2.14) at the 2σ level.

3.1 Method to Find Model Parameters and Examples

We have learned that the location of the plateau, i.e. ϕ_0 , is determined by the parameter A of the rewritten potential (2.7); we treat it as a free parameter. The slope of the plateau is determined by β , i.e. for given field value (not too far from ϕ_0) the SR parameter ϵ_V will become larger when β is increased. Of course, the SR parameters, as well as N_{CMB} and r , also depend on ϕ_{CMB} . On the other hand, the overall coupling d in eq.(2.7) only affects the normalization of the power spectrum, see eq.(2.10).

In practice we first fix ϕ_0 . The parameters ϕ_{CMB} and β should then be chosen such that n_s and N_{CMB} have the desired values. As argued in the previous subsection, viable solutions only exist for $\phi_{\text{CMB}} < \phi_0$. Reducing ϕ_{CMB} for given β means that one is moving away from the flattest part of the potential (apart from the region near the minimum, which cannot lead to inflation); this increases ϵ_V and reduces η_V (often making it more negative). This means that $1 - n_s$ and r both increase when ϕ_{CMB} is reduced, but N_{CMB} becomes smaller. Reducing β for fixed ϕ_{CMB} has the opposite effect: the potential becomes flatter, which increases N_{CMB} but decreases r and usually also $1 - n_s$.

For $\phi_0 \lesssim 5$ the approximation described by eqs.(2.15)–(2.21) still works fairly well. As already noted in the corresponding discussion, in this case one can use the spectral slope n_s to determine ϕ_{CMB} , and then chose β such that N_{CMB} is reproduced. For this range of parameters r is still very small, well below the present bound.

This procedure yields $1 - \phi_{\text{CMB}}/\phi_0 \propto \phi_0^2$, so the approximation $\phi_0 - \phi_{\text{CMB}} \ll \phi_0$ begins to break down for $\phi_0 \geq 5$. The free parameters ϕ_{CMB} and β then need to be determined together. We find that this can still be done iteratively. One starts with a guess for β , e.g. the small- ϕ_0 value $\simeq 10^{-6}\phi_0^4$. For this value of β , ϕ_{CMB} is selected such that the spectral index n_s comes out as desired. One then fixes ϕ_{CMB} and varies β until N_{CMB} takes the desired value. With this new value of β , a new value of ϕ_{CMB} can be computed using n_s , and so on. This iteration usually converges fairly quickly. At the end, the overall coupling strength d is determined using eq.(2.10) with $\mathcal{P}_\zeta = 2.1 \cdot 10^{-9}$.

Of course, one should also check that r and the running of the spectral index α have acceptable values. We find that α is always negative, and lies within the currently allowed range given in (2.13). On the other hand, for large ϕ_0 the tensor-to-scalar ratio r may come out too large. Moreover, while for sufficiently small ϕ_0 the desired values of n_s and N_{CMB} can always be attained, this is not necessarily true for larger values of ϕ_0 .

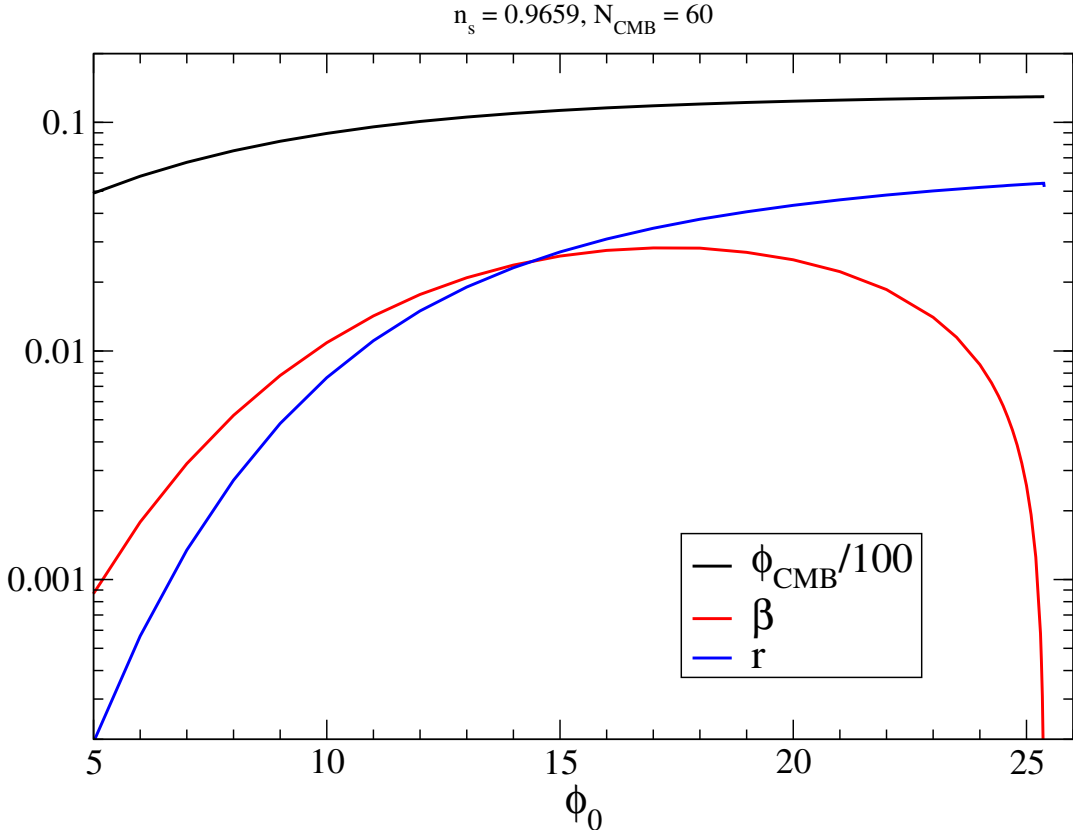


Figure 2: The values of ϕ_{CMB} (black, divided by 100) and β (red) that lead to $n_s = 0.9659$ and $N_{\text{CMB}} = 60$, as function of ϕ_0 . The blue curve shows the resulting prediction for the tensor-to-scalar ratio r .

This procedure is illustrated in Fig. 2, for $\phi_0 \geq 5$ where the deviation from the small- ϕ_0 solution begins to be sizable. Here we have chosen $N_{\text{CMB}} = 60$ and $n_s = 0.9659$, the current central value. We see that for $\phi_0 \lesssim 10$, ϕ_{CMB} (shown in black) has to remain quite close to ϕ_0 . For fixed ratio ϕ_{CMB}/ϕ_0 an increase of ϕ_0 reduces the SR parameters due to the overall $1/\phi^2$ factors in eqs.(2.8), moving n_s closer to 1. This has to be compensated by decreasing ϕ_{CMB}/ϕ_0 . On the other hand, N_{CMB} depends not only on the SR parameter ϵ_V , but also on the range of field values over which the integral in eq.(2.9) has to be evaluated. An increase of ϕ_0 thus has to be compensated by an increase in β , shown by the red curve, in order to leave N_{CMB} unchanged. This leads to a rapid increase of ϵ_V , and hence of r (shown in blue); however, in this region of parameter space we still have $\epsilon_V \ll |\eta_V|$, i.e. the spectral index n_s is essentially determined by η_V .

For $\phi_0 > 10$ the curve for ϕ_{CMB} flattens out. Recall that even for a purely quadratic potential $\phi_{\text{CMB}} \simeq 15$, see eq.(2.27), and our potential is significantly flatter, hence requiring smaller ϕ_{CMB} in order to give the correct N_{CMB} . At the same time ϵ_V keeps increasing, so that its contribution to n_s becomes significant. This flattens the increase of β , which reaches

a maximum at $\phi_0 \simeq 17$. For yet larger values of ϕ_0 , ϕ_{CMB} becomes almost independent of ϕ_0 , i.e. inflation now occurs further and further away from the saddle point. Keeping the potential sufficiently flat then requires a *reduction* of β . For the given choice of n_s and N_{CMB} no solution can be found for $\phi_0 \geq 25.4$; the red curve drops very steeply at the end, since the potential at $\phi_{\text{CMB}} \sim 0.55\phi_0$ depends only weakly on the slope at ϕ_0 .

Note that r keeps increasing even when β is decreasing; for the chosen parameters, it exceeds the bound of 0.035 for $\phi_0 \geq 17.5$. However, for other choices of $N_{\text{CMB}} \in [50, 65]$ and $n_s \in [0.9579, 0.9739]$ (the 2σ range) the solution terminates before the bound on r is saturated.⁸ Notice also that β remains quite small throughout, i.e. the potential indeed needs to feature a near-inflection point.

In Table 1 we explore a wider range⁹ of N_{CMB} and n_s , for ϕ_0 between 1 and 20. The overall trends are as in Fig. 2: ϕ_{CMB} remains close to ϕ_0 for $\phi_0 \lesssim 10$, but increases only slowly once $\phi_0 > 15$; and β at first increases quickly, but reaches a maximum at ϕ_0 around 15 and then quickly diminishes again. We also see that the model can saturate the upper bound on r for $\phi_0 \geq 14$.

Moreover, the running α of the spectral index is always negative, and well within the currently allowed range given in (2.13). It is essentially independent of ϕ_0 for $\phi_0 \lesssim 5$, but becomes smaller in magnitude for $\phi_0 \geq 8$. In fact, ξ_V^2 changes sign at $\phi_{\text{CMB}} = 2\phi_0(1 - \beta)/3$; for the parameters used in Fig. 2 this happens at $\phi_0 \simeq 18$. However, by then ϵ_V has become so large that the first two terms in the expression for α in eq.(2.11) dominate; these terms are negative since $\eta_V < 0$.

Table 1 also lists the values of d needed to reproduce the observed normalization of the spectrum of CMB anisotropies, computed from eq.(2.10). At small ϕ_0 the coupling scales like $d \propto \phi_0^2$, since $V(\phi_{\text{CMB}}) \propto d\phi_0^4$ and $\epsilon_V \propto \phi_0^6$. However, for $\phi_0 > 5$ the growth of ϵ_V with increasing ϕ_0 slows down. As a result, d reaches a maximum value near 10^{-13} at $\phi_0 \sim 10$, and decreases again for yet larger values of ϕ_0 . As a result, the physical inflaton mass $m_\phi = 2\sqrt{d}\phi_0$ increases $\propto \phi_0^2$ for $\phi_0 \lesssim 5$, but depends only weakly on ϕ_0 for $\phi_0 > 10$.

3.2 Complete Scan of Parameter Space

In order to explore the full parameter space, we scan over the parameters ϕ_0 , ϕ_{CMB} and β ; d has again been fixed such that $\mathcal{P}_\zeta \simeq 2.1 \cdot 10^{-9}$. We accept all combinations of parameters that yield $50 \leq N_{\text{CMB}} \leq 65$ and satisfy the constraints on n_s and r shown in Fig. 1. We see from Fig. 3 that this scan in fact fills the entire presently allowed region of the (n_s, r) plane.

The allowed ranges of the model parameters and the resulting predictions for r , n_s and N_{CMB} are further shown as function of ϕ_0 in Fig. 4.

The upper left panel shows ϕ_{CMB} . For $\phi_0 \lesssim 5$, $\phi_{\text{CMB}} \simeq \phi_0$ can be analytically obtained by [49]

$$\phi_{\text{CMB}} = \phi_0(1 - \delta_{\text{CMB}}) \simeq \phi_0(1 - 7.10 \cdot 10^{-4}\phi_0^2); \quad (3.1)$$

here we have used $\delta_{\text{CMB}} \simeq 1 - \frac{\phi_0^2}{48}(1 - n_s)$ (cf. Eq.(2.19)) with $n_s = 0.9659$. This analytical approximation is shown by the red line, which describes the numerical results very well for

⁸As long as only field values below ϕ_0 are considered, one could find additional solutions with larger ϕ_0 and negative β . Recall, however, that in this case the potential features a second minimum above ϕ_0 , in which the inflaton would get stuck if it came from yet larger field values; in particular, in scenarios featuring a phase of eternal inflation, as discussed below. This is why we restrict ourselves to $\beta \geq 0$.

⁹Generically $N_{\text{CMB}} < 65$ unless there is an exotic reheating phase following the end of inflation [51, 52]. For our case, inflation ends with a usual quadratic potential, hence we adopt $50 \leq N_{\text{CMB}} \leq 65$.

ϕ_0	$d/10^{-14}$	$\beta/10^{-3}$	ϕ_{CMB}	n_s	$r/10^{-3}$	$\alpha/10^{-3}$	N_{CMB}
1	0.00636	0.0009	0.999203	0.9619	$6.81 \cdot 10^{-6}$	-1.40	64.6
1	0.164	0.0017	0.999285	0.9659	$1.76 \cdot 10^{-5}$	-2.24	54.6
1	0.268	0.0023	0.999368	0.9699	$2.87 \cdot 10^{-5}$	-2.87	50.2
2	0.27	0.015	1.99356	0.9619	$4.64 \cdot 10^{-4}$	-1.43	64.3
2	0.65	0.027	1.99418	0.9659	$1.11 \cdot 10^{-3}$	-2.22	55.2
2	1.03	0.036	1.99482	0.9699	$1.77 \cdot 10^{-3}$	-2.80	51.1
3	0.66	0.08	2.97783	0.9619	$5.74 \cdot 10^{-3}$	-1.47	63.8
3	1.52	0.14	2.97976	0.9659	$1.32 \cdot 10^{-2}$	-2.24	55.2
3	2.49	0.19	2.98175	0.9699	$2.17 \cdot 10^{-2}$	-2.87	50.7
4	1.16	0.25	3.9461	0.9619	$3.18 \cdot 10^{-2}$	-1.43	64.4
4	2.77	0.45	3.9499	0.9659	$7.62 \cdot 10^{-2}$	-2.22	55.2
4	4.39	0.60	3.9542	0.9699	$1.21 \cdot 10^{-1}$	-2.81	51.0
5	2.23	0.7	4.8899	0.9619	0.15	-1.55	61.9
5	4.29	1.1	4.8968	0.9659	0.29	-2.16	55.2
5	7.02	1.5	4.9037	0.9699	0.48	-2.77	50.6
8	4.54	4.0	7.4815	0.9619	2.04	-1.23	62.3
8	8.76	6.7	7.4879	0.9659	4.01	-1.72	55.0
8	13.05	9.0	7.5048	0.9699	6.07	-2.12	51.2
11	5.19	10	9.4906	0.9619	8.5	-0.84	62.1
11	9.43	19	9.4772	0.9659	16.1	-1.18	54.7
11	11.99	25	9.5432	0.9699	21.1	-1.35	52.7
14	6.93	26	10.6090	0.9619	29.8	-0.82	53.7
14	7.05	33	10.8235	0.9659	31.5	-0.83	55.3
14	7.36	41	11.0439	0.9699	34.2	-0.86	56.6
17	3.28	8	11.6109	0.9619	27.1	-0.49	61.1
17	3.43	22	11.8913	0.9659	30.0	-0.51	62.6
17	3.73	39	12.1859	0.9699	34.9	-0.55	63.6
20	2.25	3	12.4500	0.9651	32.9	-0.42	64.3
20	2.28	8	12.5183	0.9659	33.9	-0.42	64.6
20	2.30	13	12.6000	0.9668	34.7	-0.43	65.0

Table 1: Examples of model parameters and corresponding predictions. The overall coupling strength d has been chosen to reproduce the central value of power spectrum, i.e. $\mathcal{P}_\zeta \simeq 2.1 \cdot 10^{-9}$. The predictions for n_s and α are consistent with Planck 2018 results (2.13) at the 1σ level. Predictions for the tensor-to-scalar ratio r satisfy the current bound $r < 0.035$ (from the recent BICEP/Keck 2018 [8]) and range from $\mathcal{O}(10^{-8})$ to $\mathcal{O}(10^{-2})$.

small ϕ_0 . As we already saw in Fig. 2, this approximation breaks down for $\phi_0 > 5$, where the difference between ϕ_0 and ϕ_{CMB} increases quickly. Eventually ϕ_{CMB} becomes nearly independent of ϕ_0 , taking values around 12; larger ϕ_{CMB} would require larger ϵ_V in order to keep N_{CMB} within the acceptable range, in conflict with the upper bound on r .

The middle left panel of Fig. 4 gives β as function of ϕ_0 . Here the analytical small ϕ_0 approximation gives [49]

$$\beta \simeq 1.65 \cdot 10^{-6} \phi_0^4, \quad (3.2)$$

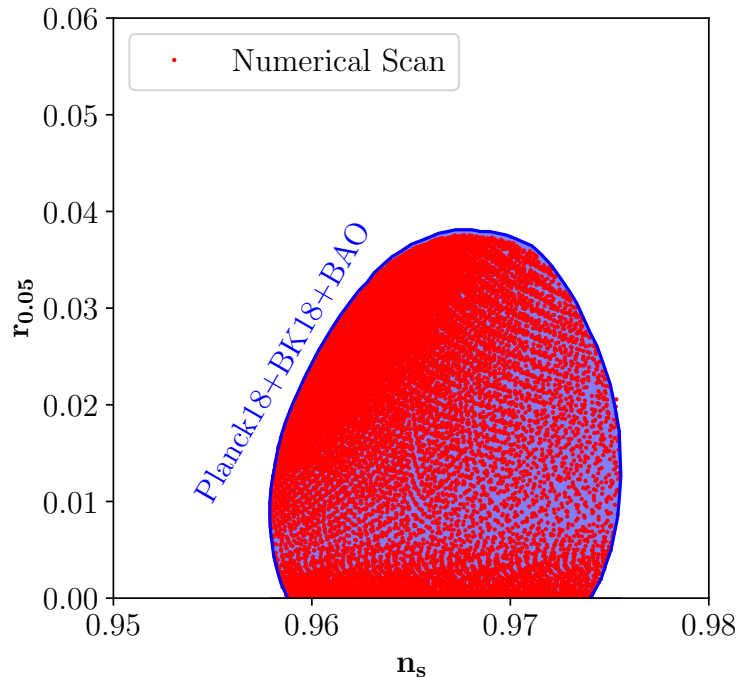


Figure 3: The numerical scan over the free parameters ϕ_0 , ϕ_{CMB} and β , requiring $50 \leq N_{\text{CMB}} \leq 65$, fills the entire allowed region of the (n_s, r) plane.

for our choices $N_{\text{CMB}} = 55$ and $n_s = 0.9659$; again, this reproduces the numerical results for $\phi_0 \lesssim 5$. On the other hand, for $\phi_0 \geq 15$, a relatively wide range of values of β is allowed, since for $\beta \ll 1$ the potential at $\phi \lesssim \phi_{\text{CMB}}$ only weakly depends on β ; recall from the top-left frame that $\phi_{\text{CMB}} \leq 0.7\phi_0$ lies well below the near-inflection point for these large values of ϕ_0 .

The lower left panel of Fig. 4 shows d as function of ϕ_0 . In this case the small ϕ_0 approximation yields [49]

$$d \simeq 1.55 \cdot 10^{-15} \phi_0^2, \quad (3.3)$$

for $\mathcal{P}_\zeta = 2.1 \cdot 10^{-9}$ and our default values of n_s and N_{CMB} .¹⁰ On the other hand, we already saw in the discussion of Table 1 that for $\phi_0 > 10$, a smaller coupling d is required in order to obtain the correct power spectrum.

The upper right panel of Fig. 4 depicts r as function of ϕ_0 . For $\phi_0 \lesssim 5$ this is again quite well described by the analytical approximation [49]

$$r \simeq 1.66 \cdot 10^{-8} \phi_0^6. \quad (3.4)$$

For $\phi_0 > 5$ r increases slightly less quickly with increasing ϕ_0 ; nevertheless for $\phi_0 \gtrsim 12$ solutions can be found that saturate the current upper bound on r . In fact, for $\phi_0 > 22$ *all* solutions that give $N_{\text{CMB}} \leq 65$ predict too large a value of r .

¹⁰The larger scatter of the blue points around the red curve in this frame, compared to the top left and middle left frames, is largely a plotting artifact. The y -axis in the latter spans 6 orders of magnitude compared to “only” 4 orders of magnitude in the lower left frame, making the blue “bars” appear correspondingly shorter. Moreover, for $\phi_0 \lesssim 5$ the dynamics is more usefully described by the scaled difference δ introduced in eq.(2.15); the scatter in δ_{CMB} for $\phi_0 \lesssim 5$ is similar to that in β and d .

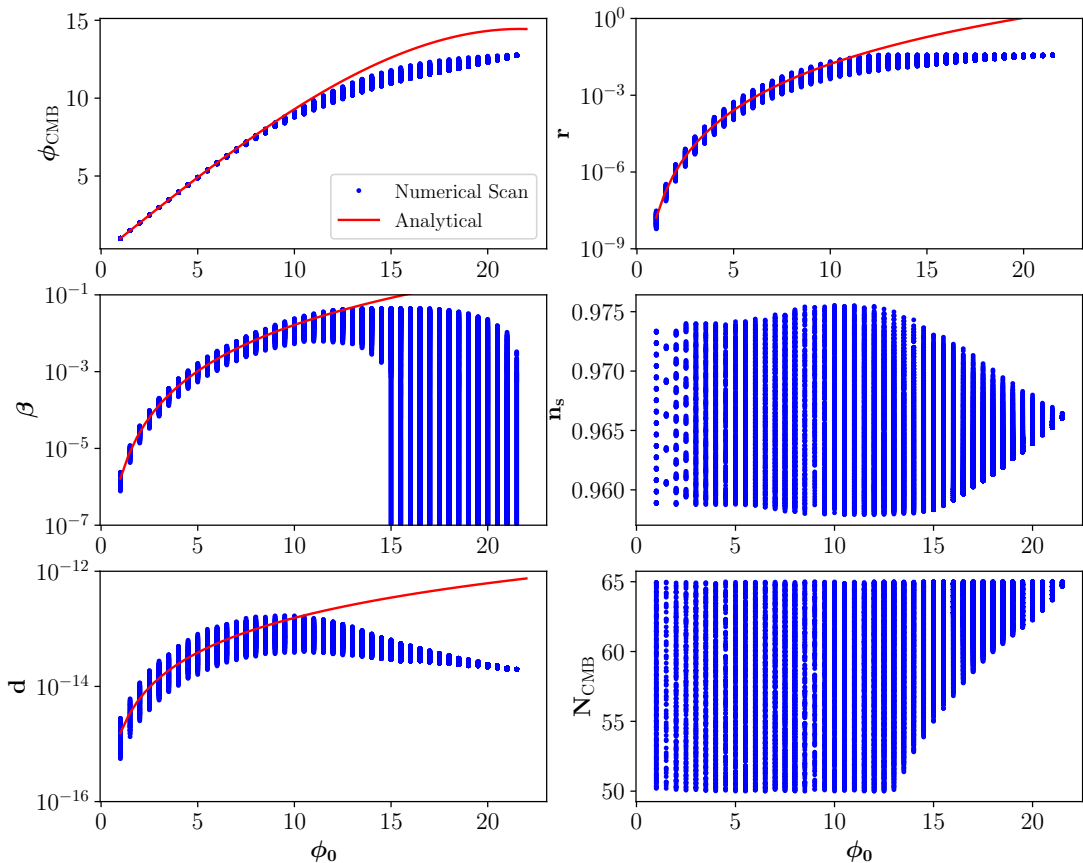


Figure 4: Blue dots represent allowed sets of model parameters (left frames) and the corresponding predictions (right frames) using the full expressions. The red lines depict the analytical approximation valid for $\phi_0 - \phi_{\text{CMB}} \ll \phi_0$, for fixed $n_s = 0.9659$ and $N_{\text{CMB}} = 55$, as described in the text.

The middle right panel of Fig. 4 gives n_s as function of ϕ_0 . For $\phi_0 \leq 13$ essentially the entire currently allowed range can be covered by our model. For larger values of ϕ_0 the parameter space begins to get squeezed by the conflicting constraints $N_{\text{CMB}} \leq 65$ and $r \leq 0.035$. Probably coincidentally the prediction of n_s for the largest allowed ϕ_0 is quite close to the present central value.

Finally, the lower right panel of Fig. 4 gives results for N_{CMB} . Again for $\phi_0 \leq 13$ all values between our chosen limits of 50 and 65 can be reproduced. For larger ϕ_0 the upper bound on r leads to a lower bound on N_{CMB} , since a flatter potential reduces the former but increases the latter. As we saw above, the two constraints become incompatible for $\phi_0 > 22$.

Let us end this section by summarizing the parameter space for the polynomial inflation model (2.7):

$$6 \cdot 10^{-16} \lesssim d \lesssim 2 \cdot 10^{-13}; \quad 0 < \beta \lesssim 4 \cdot 10^{-2}; \quad \phi_0 \lesssim 21.5. \quad (3.5)$$

The upper bound on ϕ_0 immediately yields a lower bound on the cubic potential parameter, $A \gtrsim -57$. Recall that these limits have been derived from the observed value of n_s , the constraint on N_{CMB} , and the upper bound on r . It might be worth mentioning that in our

model the constraint on n_s suffices to derive a theoretical upper bound on the tensor-to-scalar ratio, $r \lesssim 0.06$, if $N_{\text{CMB}} \gtrsim 60$; however, for $N_{\text{CMB}} \lesssim 55$ significantly larger values of r could have been reproduced. The recent bound on r therefore significantly reduces the allowed parameter space of our model. The above discussion also shows that a tighter upper bound on r would further limit the parameter space; in particular, the upper bound on ϕ_0 would become smaller if next-generation experiments fail to detect CMB tensor modes.

4 Radiative Stability and Reheating

So far our analysis has been based on the tree-level potential (2.7). This is only justified if loop corrections to the potential are small. In order to check this one can compute the 1-loop Coleman–Weinberg (CW) corrections to the potential [53] and require that they are subdominant compared to the tree-level potential. Here we follow the procedure outlined in Ref. [49]. In particular, we focus on the potential at ϕ_0 . Here the first and second derivatives of the tree-level potential are suppressed by the small parameter β , which increases the relative importance of loop corrections.

The bound on the inflaton self-coupling can be computed by requiring the second derivative of the 1-loop potential at $\phi = \phi_0$ to be comparable to the tree-level value. This gives

$$\left| \frac{d^2 \ln(16d\beta)}{\pi^2} \right| < 8d\beta. \quad (4.1)$$

Since for $\phi_0 \geq 1$ we typically have $\beta \gtrsim 10^{-6}$ while $d \lesssim 10^{-13}$, this inequality is nearly always satisfied. As shown in Fig. 4, for $\phi_0 \gtrsim 14.5$, β can in principle become arbitrarily small. However, the inflationary parameters basically do not change when β is increased from, say, 10^{-15} to a loop corrected value of 10^{-13} ; our predictions therefore remain stable in this part of parameter space even if the inequality (4.1) is violated. This therefore does not lead to an additional theoretical constraint on the parameter space, in contrast to the small-field version of this model [49].

4.1 Reheating

In a complete model of very early universe cosmology the inflaton field has to couple to external particles for reheating [50, 54]. Here we assume ϕ couples to daughter particles with trilinear couplings in order to fully drain the inflaton energy so that a radiation dominated epoch is reproduced after reheating. For a scalar field ϕ' , e.g. the standard model Higgs field, we introduce a term $g\phi|\phi'|^2$ in the Lagrangian; for a fermionic field χ , e.g. right-handed neutrino, the corresponding term is $y\phi\bar{\chi}\chi$.¹¹ The radiative stability conditions [49]

¹¹The non-perturbative preheating effect in our model is negligible. In the bosonic case, i.e. preheating with Higgs production, the trilinear coupling induce tachyonic instabilities [55], which tends to make preheating efficient. However the Higgs self-coupling gives rise to a positive effective mass $\propto \lambda_{\phi'} \langle \phi'^2 \rangle$ (where $\lambda_{\phi'} \sim \mathcal{O}(0.1)$ is the Higgs self-coupling and $\langle \phi'^2 \rangle$ denotes the variance of the produced Higgs field), which quickly dominates over the (possibly negative) contribution $\propto g\phi$ (where the small trilinear coupling g is bounded by Eq. (4.5)), thereby blocking further non-perturbative $\phi \rightarrow \phi'$ energy transfer [49, 56]. In the fermionic case, Pauli blocking implies that only a small fraction of the energy stored in the inflaton field can be non-perturbatively transferred to χ particles, unless the daughter particles decay very fast [57].

then read:

$$\left| \frac{y^4 - 3y^4 \ln(y^2)}{4\pi^2} \right| < 16d\beta; \quad (4.2)$$

$$\frac{1}{8\pi^2} \left(\frac{g}{\phi_0} \right)^2 \left| \ln \left(\frac{g}{\phi_0} \right) - 1 \right| < 8d\beta. \quad (4.3)$$

For typical value of $d \sim 10^{-14}$ and $\beta \lesssim \beta_{\max} \simeq 4 \cdot 10^{-2}$ (cf. Eq. (3.5)), one has

$$y \lesssim y_{\max} \simeq 2.7 \cdot 10^{-4}; \quad (4.4)$$

$$\left(\frac{g}{\phi_0} \right) \lesssim \left(\frac{g}{\phi_0} \right)_{\max} \simeq 1.2 \cdot 10^{-7}. \quad (4.5)$$

These upper bounds on the inflaton couplings immediately lead to upper bounds on the corresponding partial widths for $\phi \rightarrow \phi'\phi'$ and $\phi \rightarrow \bar{\chi}\chi$ decays, which in turn imply upper bounds on the post-inflationary reheating temperature. In the instantaneous decay approximation the latter is given by [54]

$$T_{\text{rh}} \simeq 1.41 g_{\star}^{-1/4} \Gamma_{\phi}^{1/2}. \quad (4.6)$$

For the fermionic reheating channel, this becomes

$$T_{\text{rh}}^{\chi} \simeq 1.41 g_{\star}^{-1/4} \left(2\phi_0 \frac{y^2}{8\pi} \sqrt{d} \right)^{1/2} \lesssim 1.1 \cdot 10^{11} \text{ GeV}, \quad (4.7)$$

where we have considered $\phi_0 \lesssim 20$, $g_{\star} = 106.75$ and used Eq. (4.4) for the upper bound on y . For bosonic reheating, the analogous calculation allows even higher reheat temperatures,

$$T_{\text{rh}}^{\phi'} \simeq 1.41 g_{\star}^{-1/4} \left(\frac{g^2}{8\pi 2\phi_0 \sqrt{d}} \right)^{1/2} \lesssim 2.5 \cdot 10^{14} \text{ GeV}, \quad (4.8)$$

where the maximum value g_{\max} reported in Eq. (4.5) has been utilized.

Both bounds are saturated at the largest allowed value of ϕ_0 , where the physical mass of the inflaton $m_{\phi} = 2\sqrt{d}\phi_0 \simeq 10^{13}$ GeV. This is comfortably above the bound (4.7), which can thus be saturated using simple perturbative $\phi \rightarrow \chi\bar{\chi}$ decays. On the other hand, m_{ϕ} is an order of magnitude below the bound (4.8). This bound can therefore only be saturated if one can turn an ensemble of ϕ' particles with energy $\simeq m_{\phi}/2 \sim 5 \cdot 10^{12}$ GeV into a thermal bath with much higher temperature, which can only happen via scattering reactions that *reduce* the number of particles, in particular $3 \rightarrow 2$ scattering reactions. It is not clear whether the rate of such reactions is sufficiently high that the bound (4.8) can be saturated; in the absence of such reactions it would have to be replaced by $T_{\text{rh}}^{\phi'} \lesssim m_{\phi}/2$. The same remark holds for the maximal temperature of the radiation bath, which is typically attained well before reheating is completed and can be significantly larger than T_{rh} [54]: in the absence of fast $3 \rightarrow 2$ reactions it is also bounded by $m_{\phi}/2$.

5 Eternal Polynomial Inflation

In the previous sections, we have worked out the parameter space consistent with Planck 2018 (2.13) and BICEP/Keck 2018 (2.14) and investigated the radiative stability of the inflaton potential as well as perturbative reheating for the polynomial inflation model. All this happened at field values (well) below ϕ_0 . In this section we analyze the situation at $\phi \gtrsim \phi_0$. In particular, we are interested in the energy scale(s) at which “eternal” inflation could have occurred within the allowed parameter space.

5.1 Eternal Phase I

During the SR phase, one can neglect the acceleration term in eq. (2.2), so that the classical inflaton field evolves as

$$\dot{\phi} \approx -\frac{V'(\phi)}{3H}. \quad (5.1)$$

This predicts a classical field excursion per Hubble time

$$\Delta\phi_{\text{cl}} = \frac{|\dot{\phi}|}{H} \approx \frac{|V'(\phi)|}{3H^2} \approx \frac{|V'(\phi)|}{V} = \sqrt{2\epsilon_V}. \quad (5.2)$$

On the other hand, since the inflaton field is very weakly coupled its quantum fluctuations follow a Gaussian probability distribution. In the quasi de Sitter background during SR inflation, the typical size of these quantum fluctuation over one Hubble time is given by $\delta\phi_{\text{qu}} = \frac{H}{2\pi}$ [58, 59].

Assume that the quantum fluctuation dominates over the classical field excursion, i.e. $\delta\phi_{\text{qu}} > \Delta\phi_{\text{cl}}$. In this case the inflaton field in a given Hubble volume is almost as likely to move “uphill”, towards larger values, as it is to move towards the minimum of the potential. Since after a small number of e-folds of inflation the inflaton field fills a great many Hubble volumes which henceforth evolve independently, it is virtually guaranteed that in some of these volumes the field does indeed move uphill. Since these regions subsequently will expand faster (owing to the larger Hubble parameter), in this picture “most” of space will continue inflating forever, even though inflation clearly must have ended in our own Hubble patch. This is known as eternal inflation.

From eq.(5.2) and $\delta\phi_{\text{qu}} = \frac{H}{2\pi}$, the condition for eternal inflation is

$$\frac{H}{2\pi} > \sqrt{2\epsilon_V} \Leftrightarrow \frac{H^2}{8\pi^2\epsilon_V} > 1. \quad (5.3)$$

Hence the condition for eternal inflation is satisfied if the leading order prediction of the amplitude of curvature perturbations \mathcal{P}_ζ exceeds unity [38].

As already emphasized in sec. 2.2, for $\phi \gg \phi_0$ effectively our model behaves like quartic inflation, i.e. the inflaton potential can be simplified to $V = d\phi^4$, so that

$$H = \sqrt{\frac{d}{3}}\phi^2, \quad (5.4)$$

and

$$\frac{H^2}{8\pi^2\epsilon_V} = \frac{d\phi^6}{192\pi^2}. \quad (5.5)$$

From condition (5.3) eternal inflation then requires

$$\phi^2 > \left(\frac{192\pi^2}{d}\right)^{1/3}. \quad (5.6)$$

This in turn leads to a lower bound on the Hubble parameter:

$$H > H_{\text{EI}}^c = 4\pi^{2/3} \left(\frac{d}{3}\right)^{1/6}, \quad (5.7)$$

which only depends on d . Once $H > H_{\text{EI}}^c$, an eternal inflationary phase can occur.

The usual monomial chaotic $\lambda\phi^4$ inflation model requires $\lambda \sim 10^{-12}$ [33] in order to match the normalization of the power spectrum; eq. (5.7) then yields $H_{\text{EI}}^c \approx 0.07$. In the last section we saw that in our polynomial scenario the quartic coupling d needs to be somewhat smaller, $6 \cdot 10^{-16} \lesssim d \lesssim 2 \cdot 10^{-13}$. The corresponding threshold value of the inflaton field is (in Planckian units):

$$460 \lesssim \phi_c \lesssim 1211, \quad (5.8)$$

which evidently is indeed well above ϕ_0 . One can further work out the threshold of the corresponding inflationary scale (again in Planckian units):

$$0.02 \lesssim H_{\text{EI}}^c \lesssim 0.05. \quad (5.9)$$

Evidently the corresponding energy scale is well below the Planck scale (and also somewhat below the scale required for eternal inflation in pure quartic inflation); hence our semi-classical treatment, which ignores “quantum gravity” effects, may be valid.

We thus conclude that our model does allow for an epoch of “eternal” while reproducing all present measurements of inflationary parameters.

5.2 Eternal Phase II

The discussion in the previous section shows that eternal inflation should occur in the polynomial model if the inflaton field and the Hubble parameter ever exceeded the critical values (5.8) and (5.9), respectively. Here we show that, at least in part of the allowed parameter space, a second, later epoch of eternal inflation will occur.

We have seen in Fig. 4 that the parameter β can be arbitrarily small if $\phi_0 \gtrsim 15$. Recall that a very small β implies that the potential at ϕ_0 is very flat. Hence it is expected that a (second) eternal phase can occur. Since this eternal phase appears when the inflaton is near the saddle point ϕ_0 , which is much smaller than ϕ_c analyzed above, one can expect that the corresponding Hubble scale should be much lower than H_{EI}^c of eq.(5.9).¹²

In order to obtain the maximum value of β that allows a second phase of eternal inflation, we again use condition Eq. (5.3), identical to the leading order prediction of the power spectrum being larger than unity as mentioned earlier. Since the potential is flattest at $\phi = \phi_0$, we can use eq.(2.18) with $\delta = 0$ to derive the condition for the existence of a second epoch of eternal inflation:

$$\beta < \frac{\sqrt{d}\phi_0^3}{144\pi} \simeq 10^{-6}; \quad (5.10)$$

For the numerical value we have used $d \sim 10^{-14}$ and $\phi_0 \sim 20$.

The potential at ϕ_0 is given by $d\phi_0^4/3$, up to corrections of relative order β which are evidently completely negligible here. This epoch of eternal inflation would thus have a Hubble parameter

$$H_{\text{EI}} = \frac{\sqrt{d}}{3}\phi_0^2 \sim 10^{-5}; \quad (5.11)$$

¹²This has some similarity to eternal hilltop inflation investigated in [38]. However, in our case the inflaton first rolls down to a plateau around the saddle point; in hilltop inflation, one has to impose as initial condition that the inflaton starts near a (local) maximum of the potential, which can also be very flat.

this is at least three orders of magnitude smaller than the one given in eq.(5.9).

The width of this second region in field space that allows eternal inflation is also important. Again from eq.(2.18) we see that the evolution of the inflaton field will be dominated by quantum fluctuations as long as

$$\delta < \delta_c = \frac{d^{1/4} \phi_0^{3/2}}{6\sqrt{2\pi}}. \quad (5.12)$$

In units of the size $H_{\text{EI}}/(2\pi)$ of random walk steps the half width of the region in field space allowing eternal inflation is thus

$$\frac{\delta_c \phi_0}{H_{\text{EI}}/(2\pi)} = \sqrt{\frac{\pi}{2}} \frac{\phi_0^{1/2}}{d^{1/4}} \simeq 1.8 \cdot 10^4. \quad (5.13)$$

Given that the average excursion in a random walk is proportional to the square of the number of steps taken times the (typical) step size, starting from $\phi = \phi_0$ the field would thus typically need more than 10^8 steps to leave the region where quantum fluctuations dominate the dynamics. Moreover, half the time the random walk would end at $\phi > \phi_0(1 + \delta^c)$, in which case the classical field evolution would bring the field back into the range where quantum effects dominate. These arguments indicate that in our model indeed “most of” space would inflate eternally if ϕ ever reached the region very close to ϕ_0 and $\beta < 10^{-6}$.

A typical inflationary trajectory starting at very large field values $\phi > \phi_c$ of eq.(5.8) is shown in Fig. 5, which plots the Hubble parameter as function of the classical prediction N_{cla} of the number of e-folds that occur after the inflaton field had a certain value, given by eq.(2.9); larger N_{cla} correspond to larger ϕ . Of course, for the field ranges allowing eternal inflation, i.e. for $\phi > \phi_c$ and for $\phi \in [\phi_0(1 - \delta_c), \phi_0(1 + \delta_c)]$, the *actual* number of e-folds by which our Hubble patch expanded was likely very much larger than the classical prediction.

For field values below ϕ_c the Hubble parameter seems to drop very steeply. However, if $\phi_0 \gtrsim 4$ the SR conditions are satisfied for all $\phi \gtrsim \phi_0$; essentially deterministic inflation therefore lasts from the end of the first, high-energy stage of eternal inflation to the onset of the second epoch of eternal inflation where $\phi \simeq \phi_0$. This is in contrast to the small-field version of this model, where the SR conditions are violated for some range of field values above ϕ_0 , and inflation around ϕ_0 is always deterministic [49]. Finally, once $\phi < \phi_0(1 - \delta_c)$ inflation is deterministic again, including the last ~ 65 e-folds of inflation with $\phi \leq \phi_{\text{CMB}}$.

Recalling the results of Fig. 4, we conclude that model parameters (a subset of (3.5)) with:

$$15 \lesssim \phi_0 \lesssim 21.5; \quad 0 < \beta \lesssim \mathcal{O}(10^{-6}); \quad 2 \cdot 10^{-14} \lesssim d \lesssim 6 \cdot 10^{-14}, \quad (5.14)$$

satisfy all observational constraints and allow a second eternal inflationary phase. Note that the second eternal phase can only occur if ϕ_0 is rather large, which implies $r \sim \mathcal{O}(10^{-2})$. The part of parameter space allowing the (unusual) low scale second eternal phase can thus be tested by the next generation CMB experiments, e.g. CORE [22], AliCPT [23], LiteBIRD [24] and CMB-S4 [25], with expected sensitivity down to $r \sim \mathcal{O}(10^{-3})$.

6 Summary and Conclusions

In this paper we revisited large field inflation with a single inflaton. We investigated a model where the inflaton potential is a polynomial of degree four. Current observations then

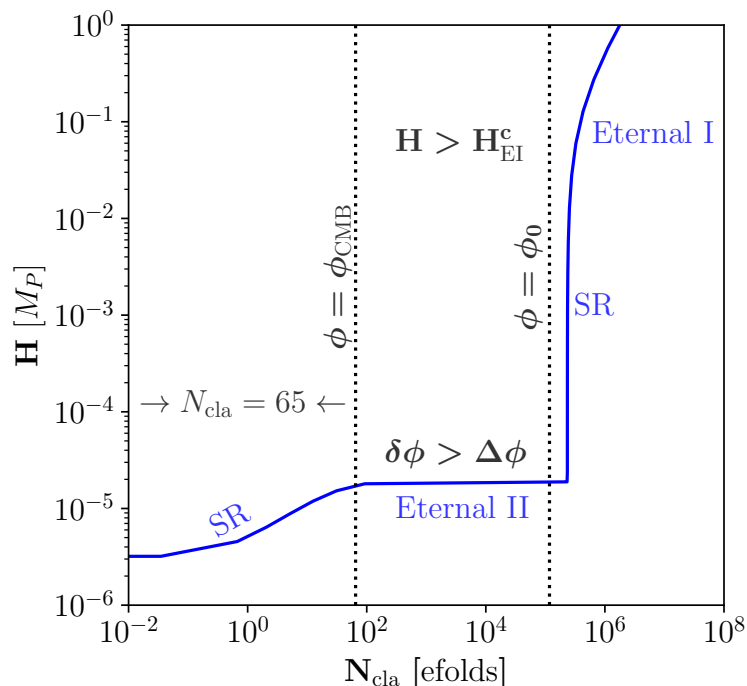


Figure 5: Evolution of the Hubble parameter as function of the classical prediction for the number of e-folds N_{cla} (depending on ϕ via Eq. (2.9)), for $\phi_0 = 20$, $\beta = 10^{-7}$ and $d \simeq 2 \cdot 10^{-14}$. Inflation can be eternal in the gray shaded region where $H > H_{\text{EI}}^c \simeq 0.04 M_{\text{Pl}}$. For $H < H_{\text{EI}}^c$ a period of the usual SR inflation follows. For the given choice of a very small β a *second* epoch of eternal inflation occurs (between the dashed vertical lines), with Hubble parameter as low as $\mathcal{O}(10^{-5}) M_{\text{Pl}}$.

require that the potential features a near saddle point at ϕ_0 , making the potential concave at $\phi \lesssim \phi_{\text{CMB}} < \phi_0$ as required by the Planck 2018 data.

The model was described in Sec. 2. The potential contains three free parameters: an overall (quartic) coupling strength d ; the location ϕ_0 of the almost saddle point; and $\beta \ll 1$ to determine the deviation from a true saddle point, with smaller β making the potential flatter for $\phi \sim \phi_0$. The parameters ϕ_0 and β thus determine the shape of the potential, while the overall normalization, given by d , can be fixed from the normalization of the power spectrum of curvature perturbation \mathcal{P}_ζ . The value ϕ_{CMB} of the inflaton field when the cosmic microwave background (CMB) scales first left the horizon is another important free parameter. It allows us to choose ϕ_0 within a rather wide range, and then use the measured spectral index n_s as well as the number N_{CMB} of e-folds of inflation generated after CMB scales first left the horizon to determine, or constrain, ϕ_{CMB} and β . We also discuss various analytical approximations. In particular, for $\phi_0 \lesssim 5$ (in Planckian units, which we use throughout) $\phi_0 - \phi_{\text{CMB}} \ll \phi_0$ and the fully analytical treatment developed for the small field version of this model [49] still holds to good approximation.

In Sec. 3 a full scan of the parameter space consistent with most recent Planck and BICEP/Keck 2018 observations at the 2σ level (cf. (2.13) and (2.14)) is described. The final result is summarized in (3.5). The predictions for r range from unobservably small, $\mathcal{O}(10^{-8})$, to the current upper bound. In fact, the current bound $r \leq 0.035$ together with the constraint

$N_{\text{CMB}} \leq 65$ leads to the upper bound $\phi_0 \lesssim 21.5$. Moreover, we predict negative running of the spectral index, $\alpha \sim -\mathcal{O}(10^{-3})$, which might be testable in the near future [60]. A large set of examples are listed in Table 1. To our knowledge, this is the first such comprehensive scan of parameter space of polynomial inflation taking into account the most recent CMB data. Of course, the currently allowed region described by eqs.(3.5), in particular the upper bound on ϕ_0 , should be further constrained once more precise CMB experiments are performed, such as CORE [22], AliCPT [23], LiteBIRD [24] and CMB-S4 [25], which could probe all $r \gtrsim \mathcal{O}(10^{-3})$.

In Sec. 4 we showed that radiative stability of the inflaton potential near the inflection-point ϕ_0 leads to relatively mild constraints for our large field model, in sharp contrast to its small field version [49]. In particular, the one-loop Coleman–Weinberg (CW) corrections to the potential due to the self-interactions of the inflaton are always harmless. Moreover, large reheat temperatures, up to 10^{11} ($2 \cdot 10^{14}$) GeV are in principle possible for perturbative inflaton decay into fermionic (bosonic) final states. However, we remind the reader that temperatures above half the inflaton mass m_ϕ can only be reached if the rate for reactions that reduce the number of particles (e.g. $3 \rightarrow 2$) is sufficiently high; note that $m_\phi \leq 10^{13}$ GeV in this model.

In Sec. 5 the possibility of eternal inflation is discussed. This is generally expected to occur in models of polynomial inflation, assuming the field value or, equivalently, the inflationary Hubble parameter reached sufficiently high values. In our case the critical Hubble parameter only depends on the size of the quartic coupling d , and lies in the range $0.02 \lesssim H_{\text{EI}}^c \lesssim 0.05$; this is somewhat below the value of 0.07 needed in the monomial $\lambda\phi^4$ model (which is in any case excluded by the upper bound on r).

More interestingly, we find that there exists another possibility to realize eternal inflation in our scenario. This occurs when the potential is very flat around ϕ_0 : for $\beta \lesssim 10^{-6}$ quantum fluctuations can dominate over the classical evolution already at $\phi \simeq \phi_0$, compared to $\phi \gtrsim \mathcal{O}(10^3)$ in the first epoch of eternal inflation. This second epoch of eternal inflation features a much smaller Hubble parameter, $H \sim \mathcal{O}(10^{-5})$, which is of the same order of magnitude as that when the CMB pivot scale $k_* = 0.05 \text{ Mpc}^{-1}$ first crossed out of the horizon. Nevertheless there will be many e-folds of deterministic inflation between the end of the second epoch of eternal inflation and the era when the CMB scales first crossed out of the horizon. We are therefore not aware of any immediate observational consequences of this “late” epoch of eternal inflation. However, since $\beta \lesssim 10^{-6}$ is possible only for $\phi_0 \gtrsim 15$, which in turn implies $r \gtrsim 0.01$, at least in our model this possibility can be tested by the next round of CMB experiments.

This novel scenario featuring two epochs of eternal inflation, as depicted in fig. 5, might also be conceptually interesting. Eternal inflation is the only known mechanism that might be able to populate the “landscape” of superstring theory [40–42]. During eternal inflation not only the inflaton field undergoes a random walk in field space, but so does *every* field whose mass is below the inflationary Hubble parameter. This might include many of the scalar fields (from the four-dimensional perspective) that determine the sizes of physical couplings in string theory. During the first, high scale epoch of eternal inflation these fields will be sampled with a typical step size $H/(2\pi) \gtrsim 5 \cdot 10^{-3}$. Since the second epoch of eternal inflation has a thousand times smaller Hubble parameter, the step size of the random walk in field space is also thousand times smaller during this second epoch. This might allow to much more efficiently “home in” on relatively small features of the landscape.

In summary, we have presented a successful large field polynomial model, worked out

the complete allowed parameter space (3.5) and offered the corresponding inflationary predictions. Combined with the earlier analysis of the small field version of this model [49] this offers the most complete analysis of the polynomial inflation model after Planck and BICEP/Keck 2018. We also pointed out for the first time that in our model the early history of the universe might feature *two* epochs of eternal inflation, at quite different energy scales.

A General Expression for the Number of e-Folds

$$\begin{aligned}
N_{\text{CMB}} &= \int_{\phi_{\text{end}}}^{\phi_{\text{CMB}}} \frac{1}{\sqrt{2\epsilon_V}} d\phi \\
&= \int_{\phi_{\text{end}}}^{\phi_{\text{CMB}}} \frac{\phi}{2} \left[\frac{32\phi^2 - 32A(\beta-1)\phi + 9A^2}{64\phi^2 - 48A(\beta-1)\phi + 9A^2} \right] d\phi \\
&= \int_{\phi_{\text{end}}}^{\phi_{\text{CMB}}} \frac{\phi}{2} \left[1 + \frac{-32\phi^2 + 16A(\beta-1)\phi}{64\phi^2 - 48A(\beta-1)\phi + 9A^2} \right] d\phi \\
&= \int_{\phi_{\text{end}}}^{\phi_{\text{CMB}}} \frac{\phi}{2} \left\{ 1 + \frac{-32\phi^2 + 16A(\beta-1)\phi}{[8\phi - 3A(\beta-1)]^2 - 9A^2(\beta^2 - 2\beta)} \right\} d\phi \\
&= \int_{\phi_{\text{end}}}^{\phi_{\text{CMB}}} \frac{\phi}{2} \left\{ 1 + \frac{-32\phi^2 + 16A(\beta-1)\phi}{64[\phi - 3/8A(\beta-1)]^2 - 9A^2(\beta^2 - 2\beta)} \right\} d\phi \tag{A.1} \\
&= \int_{\phi_{\text{end}}}^{\phi_{\text{CMB}}} \frac{\phi}{2} \left\{ 1 - \frac{1}{2} \frac{\phi^2}{[\phi + \phi_0(\beta-1)]^2 - \phi_0^2(\beta^2 - 2\beta)} - \frac{2}{3} \frac{\phi_0(\beta-1)\phi}{[\phi + \phi_0(\beta-1)]^2 - \phi_0^2(\beta^2 - 2\beta)} \right\} d\phi.
\end{aligned}$$

The three integrals can be evaluated analytically:

$$\int d\phi \frac{\phi}{2} = \frac{\phi^2}{4}; \tag{A.2}$$

$$\begin{aligned}
\int -\frac{1}{4} \frac{\phi^3}{[\phi - m]^2 + n^2} d\phi &= \frac{1}{8} \left\{ 5m^2 - 4m\phi - \phi^2 + \frac{2(m^3 - 3mn^2)}{n} \arctan \left[\frac{m - \phi}{n} \right] \right. \\
&\quad \left. - (3m^2 - n^2) \log [n^2 + (m - \phi)^2] \right\}; \tag{A.3}
\end{aligned}$$

and

$$\int \frac{1}{3} \frac{d\phi m \phi^2}{[\phi - m]^2 + n^2} = \frac{m}{3} \left\{ \phi - \frac{(m^2 - n^2)}{n} \arctan \left[\frac{m - \phi}{n} \right] + m \log [n^2 + (m - \phi)^2] \right\}, \tag{A.4}$$

with $m = \phi_0(1 - \beta)$ and $n^2 = \phi_0^2(2\beta - \beta^2)$. Combining these results, we obtain

$$\begin{aligned}
N_{\text{CMB}} &= \left\{ -\frac{m^3 + 5mn^2}{12n} \arctan \left(\frac{m - \phi}{n} \right) + \frac{5m^2}{8} - \frac{m\phi}{6} + \frac{\phi^2}{8} \right. \\
&\quad \left. - \frac{(m^2 - 3n^2)}{24} \ln [n^2 + (m - \phi)^2] \right\} \Bigg|_{\phi_{\text{end}}}^{\phi_{\text{CMB}}} \tag{A.5} \\
&\simeq \frac{1}{24} \left\{ 3\phi^2 - 4\phi\phi_0 + 15\phi_0^2 - \phi_0^2 \sqrt{\frac{2}{\beta}} \arctan \left(\frac{\phi_0 - \phi}{\sqrt{2\beta}\phi_0} \right) - \phi_0^2 \ln [(\phi_0 - \phi)^2] \right\} \Bigg|_{\phi_{\text{end}}}^{\phi_{\text{CMB}}}.
\end{aligned}$$

In the last step we have assumed $\beta \ll 1$, which is true in the allowed parameter space, but cannot be assumed a priori.

References

- [1] A.A. Starobinsky, *A New Type of Isotropic Cosmological Models Without Singularity*, *Phys. Lett.* **91B** (1980) 99.
- [2] A.H. Guth, *The Inflationary Universe: A Possible Solution to the Horizon and Flatness Problems*, *Phys. Rev. D* **23** (1981) 347.
- [3] A.D. Linde, *A New Inflationary Universe Scenario: A Possible Solution of the Horizon, Flatness, Homogeneity, Isotropy and Primordial Monopole Problems*, *Phys. Lett. B* **108** (1982) 389.
- [4] A. Albrecht and P.J. Steinhardt, *Cosmology for Grand Unified Theories with Radiatively Induced Symmetry Breaking*, *Phys. Rev. Lett.* **48** (1982) 1220.
- [5] V.F. Mukhanov and G.V. Chibisov, *Quantum Fluctuations and a Nonsingular Universe*, *JETP Lett.* **33** (1981) 532.
- [6] J. Martin, C. Ringeval and V. Vennin, *Encyclopædia Inflationaris*, *Phys. Dark Univ.* **5-6** (2014) 75 [[1303.3787](#)].
- [7] PLANCK collaboration, *Planck 2018 results. VI. Cosmological parameters*, *Astron. Astrophys.* **641** (2020) A6 [[1807.06209](#)].
- [8] BICEP/KECK collaboration, *Improved Constraints on Primordial Gravitational Waves using Planck, WMAP, and BICEP/Keck Observations through the 2018 Observing Season*, *Phys. Rev. Lett.* **127** (2021) 151301 [[2110.00483](#)].
- [9] E. Silverstein and A. Westphal, *Monodromy in the CMB: Gravity Waves and String Inflation*, *Phys. Rev. D* **78** (2008) 106003 [[0803.3085](#)].
- [10] L. McAllister, E. Silverstein and A. Westphal, *Gravity Waves and Linear Inflation from Axion Monodromy*, *Phys. Rev. D* **82** (2010) 046003 [[0808.0706](#)].
- [11] H.M. Hodges, G.R. Blumenthal, L.A. Kofman and J.R. Primack, *Nonstandard Primordial Fluctuations From a Polynomial Inflaton Potential*, *Nucl. Phys. B* **335** (1990) 197.
- [12] C. Destri, H.J. de Vega and N.G. Sanchez, *MCMC analysis of WMAP3 and SDSS data points to broken symmetry inflaton potentials and provides a lower bound on the tensor to scalar ratio*, *Phys. Rev. D* **77** (2008) 043509 [[astro-ph/0703417](#)].
- [13] G. Aslanyan, L.C. Price, J. Adams, T. Bringmann, H.A. Clark, R. Easther et al., *Ultracompact minihalos as probes of inflationary cosmology*, *Phys. Rev. Lett.* **117** (2016) 141102 [[1512.04597](#)].
- [14] R. Allahverdi, K. Enqvist, J. Garcia-Bellido and A. Mazumdar, *Gauge invariant MSSM inflaton*, *Phys. Rev. Lett.* **97** (2006) 191304 [[hep-ph/0605035](#)].
- [15] K. Nakayama, F. Takahashi and T.T. Yanagida, *Polynomial Chaotic Inflation in the Planck Era*, *Phys. Lett. B* **725** (2013) 111 [[1303.7315](#)].
- [16] K. Nakayama, F. Takahashi and T.T. Yanagida, *Polynomial Chaotic Inflation in Supergravity*, *JCAP* **08** (2013) 038 [[1305.5099](#)].
- [17] R. Kallosh, A. Linde and A. Westphal, *Chaotic Inflation in Supergravity after Planck and BICEP2*, *Phys. Rev. D* **90** (2014) 023534 [[1405.0270](#)].
- [18] T. Li, Z. Sun, C. Tian and L. Wu, *The Renormalizable Three-Term Polynomial Inflation with Large Tensor-to-Scalar Ratio*, *Eur. Phys. J. C* **75** (2015) 301 [[1407.8063](#)].
- [19] T.-J. Gao and Z.-K. Guo, *Inflection point inflation and dark energy in supergravity*, *Phys. Rev. D* **91** (2015) 123502 [[1503.05643](#)].
- [20] N. Musoke and R. Easther, *Expectations for Inflationary Observables: Simple or Natural?*, *JCAP* **12** (2017) 032 [[1709.01192](#)].

- [21] A.D. Linde and A. Westphal, *Accidental Inflation in String Theory*, *JCAP* **03** (2008) 005 [[0712.1610](#)].
- [22] CORE collaboration, *CORÉ (Cosmic Origins Explorer) A White Paper*, [1102.2181](#).
- [23] H. Li et al., *Probing Primordial Gravitational Waves: Ali CMB Polarization Telescope*, *Natl. Sci. Rev.* **6** (2019) 145 [[1710.03047](#)].
- [24] T. Matsumura et al., *Mission design of LiteBIRD*, *J. Low Temp. Phys.* **176** (2014) 733 [[1311.2847](#)].
- [25] K. Abazajian et al., *CMB-S4 Science Case, Reference Design, and Project Plan*, [1907.04473](#).
- [26] K. Enqvist, A. Mazumdar and P. Stephens, *Inflection point inflation within supersymmetry*, *JCAP* **06** (2010) 020 [[1004.3724](#)].
- [27] S. Hotchkiss, A. Mazumdar and S. Nadathur, *Inflection point inflation: WMAP constraints and a solution to the fine-tuning problem*, *JCAP* **06** (2011) 002 [[1101.6046](#)].
- [28] K. Dimopoulos, C. Owen and A. Racioppi, *Loop inflection-point inflation*, *Astropart. Phys.* **103** (2018) 16 [[1706.09735](#)].
- [29] N. Okada and D. Raut, *Inflection-point Higgs Inflation*, *Phys. Rev. D* **95** (2017) 035035 [[1610.09362](#)].
- [30] N. Okada, S. Okada and D. Raut, *Inflection-point inflation in hyper-charge oriented $U(1)_X$ model*, *Phys. Rev. D* **95** (2017) 055030 [[1702.02938](#)].
- [31] N. Okada, D. Raut and Q. Shafi, *Inflection-Point Inflation with Axion Dark Matter in light of Trans-Planckian Censorship Conjecture*, *Phys. Lett. B* **812** (2021) 136001 [[1910.14586](#)].
- [32] Y. Bai and D. Stolarski, *Dynamical Inflection Point Inflation*, *JCAP* **03** (2021) 091 [[2008.09639](#)].
- [33] A.H. Guth, *Eternal inflation and its implications*, *J. Phys. A* **40** (2007) 6811 [[hep-th/0702178](#)].
- [34] A. Vilenkin, *The Birth of Inflationary Universes*, *Phys. Rev. D* **27** (1983) 2848.
- [35] A.D. Linde, *ETERNAL CHAOTIC INFLATION*, *Mod. Phys. Lett. A* **1** (1986) 81.
- [36] E.J. Martinec and W.E. Moore, *Modeling Quantum Gravity Effects in Inflation*, *JHEP* **07** (2014) 053 [[1401.7681](#)].
- [37] L. Boubekeur and D.H. Lyth, *Hilltop inflation*, *JCAP* **07** (2005) 010 [[hep-ph/0502047](#)].
- [38] G. Barenboim, W.-I. Park and W.H. Kinney, *Eternal Hilltop Inflation*, *JCAP* **05** (2016) 030 [[1601.08140](#)].
- [39] A.D. Linde, *Eternally Existing Selfreproducing Chaotic Inflationary Universe*, *Phys. Lett. B* **175** (1986) 395.
- [40] L. Susskind, *The Anthropic landscape of string theory*, [hep-th/0302219](#).
- [41] T. Clifton, A.D. Linde and N. Sivanandam, *Islands in the landscape*, *JHEP* **02** (2007) 024 [[hep-th/0701083](#)].
- [42] A.D. Linde, *Sinks in the Landscape, Boltzmann Brains, and the Cosmological Constant Problem*, *JCAP* **01** (2007) 022 [[hep-th/0611043](#)].
- [43] A.S. Goncharov, A.D. Linde and V.F. Mukhanov, *The Global Structure of the Inflationary Universe*, *Int. J. Mod. Phys. A* **2** (1987) 561.
- [44] D.S. Goldwirth and T. Piran, *Initial conditions for inflation*, *Phys. Rept.* **214** (1992) 223.
- [45] R. Brandenberger, *Initial conditions for inflation — A short review*, *Int. J. Mod. Phys. D* **26** (2016) 1740002 [[1601.01918](#)].
- [46] A.H. Guth, *Inflation and eternal inflation*, *Phys. Rept.* **333** (2000) 555 [[astro-ph/0002156](#)].

- [47] T. Kobayashi and O. Seto, *Polynomial inflation models after BICEP2*, *Phys. Rev. D* **89** (2014) 103524 [[1403.5055](#)].
- [48] V.N. Senoguz and Q. Shafi, *Chaotic inflation, radiative corrections and precision cosmology*, *Phys. Lett. B* **668** (2008) 6 [[0806.2798](#)].
- [49] M. Drees and Y. Xu, *Small field polynomial inflation: reheating, radiative stability and lower bound*, *JCAP* **09** (2021) 012 [[2104.03977](#)].
- [50] D.H. Lyth and A.R. Liddle, *The primordial density perturbation: Cosmology, inflation and the origin of structure* (2009).
- [51] A.R. Liddle and S.M. Leach, *How long before the end of inflation were observable perturbations produced?*, *Phys. Rev. D* **68** (2003) 103503 [[astro-ph/0305263](#)].
- [52] E.H. Tanin and T. Tenkanen, *Gravitational wave constraints on the observable inflation*, *JCAP* **01** (2021) 053 [[2004.10702](#)].
- [53] S.R. Coleman and E.J. Weinberg, *Radiative Corrections as the Origin of Spontaneous Symmetry Breaking*, *Phys. Rev. D* **7** (1973) 1888.
- [54] E.W. Kolb and M.S. Turner, *The Early Universe*, vol. 69 (1990), [10.1201/9780429492860](#).
- [55] J.F. Dufaux, G.N. Felder, L. Kofman, M. Peloso and D. Podolsky, *Preheating with trilinear interactions: Tachyonic resonance*, *JCAP* **07** (2006) 006 [[hep-ph/0602144](#)].
- [56] N. Bernal and Y. Xu, *Polynomial inflation and dark matter*, *Eur. Phys. J. C* **81** (2021) 877 [[2106.03950](#)].
- [57] R. Allahverdi, A. Ferrantelli, J. Garcia-Bellido and A. Mazumdar, *Non-perturbative production of matter and rapid thermalization after MSSM inflation*, *Phys. Rev. D* **83** (2011) 123507 [[1103.2123](#)].
- [58] A.A. Starobinsky, *Dynamics of Phase Transition in the New Inflationary Universe Scenario and Generation of Perturbations*, *Phys. Lett. B* **117** (1982) 175.
- [59] A.D. Linde, *Scalar Field Fluctuations in Expanding Universe and the New Inflationary Universe Scenario*, *Phys. Lett. B* **116** (1982) 335.
- [60] J.B. Muñoz, E.D. Kovetz, A. Raccanelli, M. Kamionkowski and J. Silk, *Towards a measurement of the spectral runnings*, *JCAP* **05** (2017) 032 [[1611.05883](#)].